

SCIENTIFIC REPORTS



OPEN

Hydrolysis of Selected Tropical Plant Wastes Catalyzed by a Magnetic Carbonaceous Acid with Microwave

Received: 01 September 2015

Accepted: 02 November 2015

Published: 09 December 2015

Tong-Chao Su^{1,2}, Zhen Fang^{2,1}, Fan Zhang^{2,3}, Jia Luo² & Xing-Kang Li^{2,3}

In this study, magnetic carbonaceous acids were synthesized by pyrolysis of the homogeneous mixtures of glucose and magnetic Fe₃O₄ nanoparticles, and subsequent sulfonation. The synthesis conditions were optimized to obtain a catalyst with both high acid density (0.75 mmol g⁻¹) and strong magnetism [magnetic saturation, Ms = 19.5 Am² kg⁻¹]. The screened catalyst (C-SO₃H/Fe₃O₄) was used to hydrolyze ball-milled cellulose in a microwave reactor with total reducing sugar (TRS) yield of 25.3% under the best conditions at 190 °C for 3.5 h. It was cycled for at least seven times with high catalyst recovery rate (92.8%), acid density (0.63 mmol g⁻¹) and magnetism (Ms = 12.9 Am² kg⁻¹), as well as high TRS yield (20.1%) from the hydrolysis of ball-milled cellulose. The catalyst was further successfully tested for the hydrolysis of tropical biomass with high TRS and glucose yields of 79.8% and 58.3% for bagasse, 47.2% and 35.6% for *Jatropha* hulls, as well as 54.4% and 35.8% for *Plukenetia* hulls.

South China is located in subtropical and tropical regions that are suitable to grow energy or economic crops, such as sugarcane, *Jatropha curcas* L. and *Plukenetia volubilis* L. plants. As planned by National Development and Reform Commission of China (2015), sugar production in China will increase from 128.2 in 2013 to 180 million tons in 2020¹. As biodiesel trees, the growing area of *Jatropha* has expanded (including natural forests) to about 2 × 10⁵ ha in China². *Plukenetia* is regarded as a potential biodiesel and health food plant because of the high protein (33%) and oil (49%) contents in its seeds³, and is planned to extend its growing area by Yunnan provincial government. With the development of these tropical crops in Southern China, particularly in Yunnan, more biomass residues will be produced and it is important to volatilize them, such as conversion to sugars by hydrolysis.

A great deal of effort has been made for the hydrolysis of cellulose to glucose with enzymes, acids and supercritical water^{4,5}. The hydrolysis of lignocelluloses in concentrated and diluted homogenous acids with high sugar yield has been practiced for many years under different conditions⁶. However, problems such as corrosion hazards, acid-waste and difficulties in separation are not solved effectively. Various solid materials, such as transition metal oxides⁷, ion-exchange resins⁸, zeolites⁹ and sulfonated carbons^{10,11} are used as environmentally friendly catalysts for biomass hydrolysis because of their reusability, less corrosiveness and non-toxicity. Sulfonated carbonaceous catalysts effectively catalyze the hydrolysis of cellulose by their acidic groups such as -SO₃H, -COOH and -OH¹². Furthermore, some solid catalysts are made with magnetic design for easier separation from product mixtures^{13,14}. However,

¹University of Science and Technology of China, School of Life Science, 443 Huangshan Road, Hefei, Anhui Province, 230027, China. ²Chinese Academy of Sciences, Biomass Group, Key Laboratory of Tropical Plant Resources and Sustainable Use, Xishuangbanna Tropical Botanical Garden, 88 Xuefulu, Kunming, Yunnan Province 650223, China. ³University of Chinese Academy of Sciences, 19A Yuquan Road, Beijing 100049, China. Correspondence and requests for materials should be addressed to Z.F. (email: zhenfang@xtbg.ac.cn)

many magnetization methods are introduced by chemical reactions, such as precipitation and subsequent reduction of Fe^{3+} to Fe or Fe_3O_4 ^{4,15,16} that may cause pollution and high cost.

Moreover, many techniques are developed for biomass pretreatment to reduce the recalcitrance and crystallinity of cellulose, and increase its surface area for improving hydrolysis efficiency and selectivity. These methods include ball-milling¹⁷, liquid acid/base^{18,19}, ionic liquids²⁰ and microwave irradiation²¹ treatments. Microwave irradiation selectively heats reactants in molecular level and remarkably accelerates chemical reactions that differs from conventional heating manners such as thermal heating²².

In this study, magnetic sulfonated acid was synthesized from glucose and magnetized without chemical reactions by simply mixing magnetic Fe_3O_4 nanoparticles with aqueous glucose solution. The catalyst was screened under different conditions for optimization of glucose production from ball-milled cellulose, and further used for the hydrolysis of selected tropical biomass wastes assisted by microwave.

Methods

Materials. Nano- Fe_3O_4 ($\geq 99.5\%$, 20 nm) was purchased from Aladdin Factory Co., Ltd. (Shanghai). H_2SO_4 ($\geq 98.0\%$) and microcrystalline cellulose (powder) were purchased from Xilong Chemical Factory Co., Ltd. (Shantou, Guangdong). Standard agents glucose, xylose, arabinose, mannose, formic acid, acetic acid, lactic acid, levulinic acid, 5-hydroxymethylfurfural (HMF) and furfural (purity $\geq 99\%$) were from Sigma-Aldrich (Shanghai). Cellulose was ball-milled with ZrO_2 balls (SHQM-0.4L, Chunlong Petroleum Instrument Co., Ltd., Lianyungang, Jiangu) for 24 h before use. Bagasse was purchased from Dehong (Yunnan). *Jatropha* hulls were purchased from Yunnan Shenyu New Energy Co., Ltd. (Chuxiong, Yunnan). *Plukenetia* hulls were collected from Xishuangbanna Tropical Botanical Garden (Mengla, Yunnan). The raw materials were grounded in a pulverizer (9FC-15, Xudong machinery manufacturing Co., Ltd., Leshan, Sichuan) and dried at 45 °C until constant weight. All tropical biomass samples were sieved through 80 mesh for pretreatment and hydrolysis. Bagasse, *Jatropha* and *Plukenetia* hulls were also ball-milled for 24 h, water-extracted for 24 h, as well as water- and ethanol-extracted for 48 h at their boiling points in a Soxhlet extractor for hydrolysis.

Catalyst preparation. For a typical procedure, nano- Fe_3O_4 (2 g) and glucose (12–18 g) were mixed with 100 mL water in a three-neck flask under vigorous stirring in an oil bath at 100 °C. After water was evaporated, the mixture was transferred into a tubular furnace (SGL-1100, Shanghai Daheng Optics and Fine Mechanics Co., Ltd.), heated to 650–750 °C at rate of 5–7 °C /min and pyrolyzed for 0.5–1.5 h under N_2 flow (280 mL min^{-1}). The carbonized solid C/ Fe_3O_4 was sulfonated by 98% H_2SO_4 with the ratio of 1 g/20 mL in oil bath at 150 °C for 19–21 h. The sulfonated sample was washed repeatedly with distilled water at 200 °C for 3 h in a 50 mL high-pressure micro-autoclave (YZPR-50, Shanghai Yanzheng Experimental Instrument Co., Ltd.) until neutral solution was reached (and no SO_4^{2-} was detected using CaCl_2). The washed catalyst was dried in an oven (WFO-710, EYELA, Tokyo Rikakikai Co., Ltd.) at 105 °C for 24 h until constant weight, ground and sieved through 200 mesh for hydrolysis.

Catalyst characterization. The morphology of catalyst was examined by scanning electron microscopy (SEM, ZEISS EVO LS10, Cambridge, UK). The crystalline structure was analyzed by X-ray diffraction (XRD, Rigaku Rotaflex RAD-C, Tokyo) equipped with a Cu $\text{K}\alpha$ radiation source (40 kv and 200 mA). Fourier transform-infrared (FT-IR) measurement for catalysts and biomass was recorded on Nicolet is10 spectrometer with a spectral resolution of 4 cm^{-1} in the wavenumber range of 500–4000 cm^{-1} . The magnetism of catalyst was measured by a vibrating sample magnetometer (VSM, 7407, Lake Shore Cryotronics, Inc. Westerville, OH). The element composition of catalyst was determined by a 2400 Series II CHNS/O Elemental Analyzer (PerkinElmer, Waltham, MA), and the acid density was calculated by sulfur content. Ammonia temperature programmed desorption (NH_3 -TPD, Chemisorption analyzer, Quantachrome Instruments, Boynton Beach, FL) and NaOH titration were also used to determine the acid density. In NH_3 -TPD analysis, catalyst (20–150 mg) was treated under NH_3 flow (10% NH_3 and 90% He) for adsorption at 50 °C for 60 min after degassing, and heated to 400 °C under pure He with a heating rate of 5 °C/min for desorption. The background curve was obtained by treating catalyst under pure He instead of NH_3 flow in the adsorption step. In NaOH titration analysis, catalyst sample (0.1 g) was mixed with NaOH solution (50 mL, 0.02 mol/L) and ultrasonicated for neutralizing the surface acidity of catalyst. The consumed base concentration was back-titrated by HCl solution (0.02 mol/L) with phenolphthalein as the indicator²³.

Hydrolysis procedure. Biomass (0.027 g), a certain amount of magnetic carbonaceous acid catalyst (0.06–0.27 g) and water (about 15 mL) were loaded in a 30 mL borosilicate vial for hydrolysis in a microwave reactor (Monowave 300, Anton Paar, Graz, Austria). The vial with samples was heated to 160–200 °C (0.5–2.2 MPa) in 3 min, and reacted for 2–4 h with magnetic stirring at 600 rpm. After reaction, catalyst was separated by a magnet, washed with deionized water and dried at 105 °C for next cycles (Fig. 1). More details about the microwave experimental procedure can be seen in previous work²⁴.

The optimized conditions for ball-milled cellulose by single-factor optimization were further applied to the hydrolysis of bagasse, *Jatropha* and *Plukenetia* hulls. All experiments were repeated twice with standard deviation (σ) of 0.02–3.26% for product yields and selectivities.

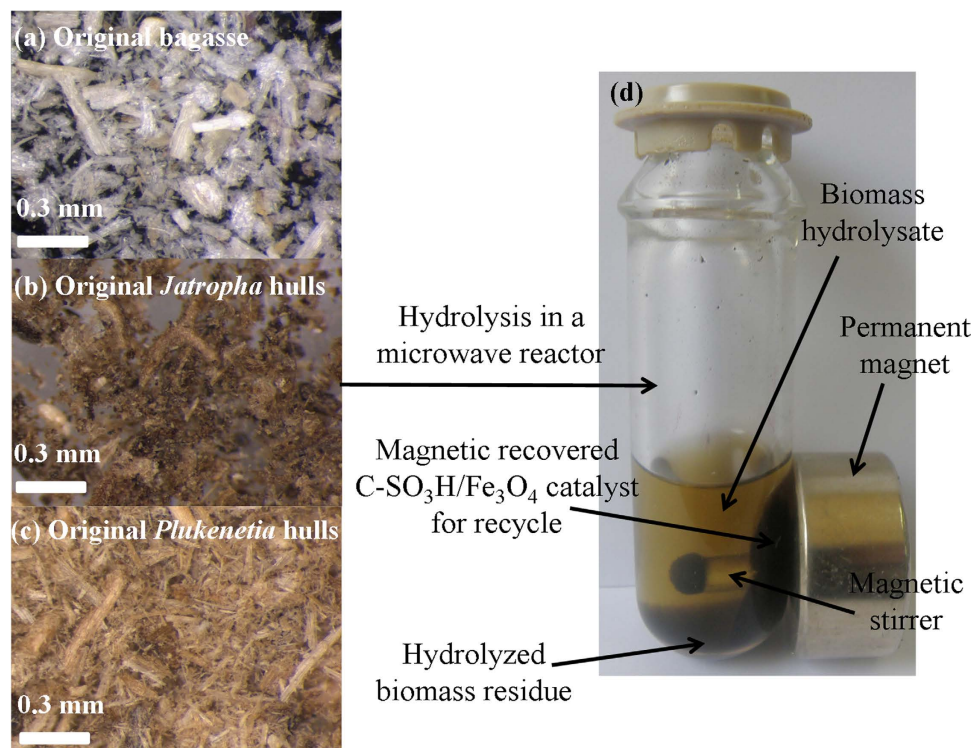


Figure 1. Photos of the tropical plant wastes and catalyst separation by a magnet after reaction.

Biomass	Glucan (%)	Xylan (%)	Arabian (%)	Mannosan (%)	Lignin (%)	Ash (%)	Extractives (%)
Bagasse	40.1 ± 2.1	18.5 ± 0.8	4.4 ± 2.3	3.2 ± 0.8	20.7 ± 3.1	3.7 ± 0.9	9.8 ± 3.1
<i>Jatropha</i> hulls	34.1 ± 1.8	10.3 ± 1.5	3.7 ± 1.3	1.0 ± 0.6	18.4 ± 2.0	3.2 ± 0.8	16.8 ± 0.6
<i>Plukenetia</i> hulls	30.5 ± 1.6	15.1 ± 0.5	2.7 ± 1.9	1.2 ± 2.5	17.3 ± 1.7	4.7 ± 2.7	17.6 ± 1.8

Table 1. Components of tropical biomass wastes (wt%)^a. ^aBy NRNL method²⁵ analyzed with 2 repeats.

Analyses of biomass wastes and hydrolysates. *Compositions of biomass wastes.* The components of the three tropical plant wastes were analyzed according to the technical report from US National Renewable Energy Laboratory (NREL)²⁵. Water-ethanol extractives fraction (wt%) was determined by total weight loss after the extraction of biomass in refluxed water for 24 h and refluxed ethanol for another 24 h at their boiling points in a Soxhlet extractor. The extracted biomass was two-step acid hydrolyzed by 72% sulfuric acid stirred in a tube at 30 °C for 1 h and subsequent by 4% sulfuric acid at 121 °C for another 1 h in a sealed tube in an autoclave (HVE-50, Hirayama Manufacturing Corp., Tokyo), with a reference standard sugar mixture (glucose, xylose, arabinose and mannose) at similar concentrations of the sugars in biomass sample for calibration the decomposition of each sugar at the second step hydrolysis. Sugar (glucose, xylose, arabinose and mannose) fractions (wt%) in hydrolysate were analyzed by high-performance liquid chromatography (HPLC) described below and quantified using a blended calibration curve with six points for each standard (excluding zero) from 0.1 to 3 mg/mL ($R^2 = 0.9999$). Acid-soluble lignin fraction (wt%) in the hydrolysate was measured by ultraviolet-visible (UV-Vis) spectrometer (UV-1800, Shimadzu, Kyoto) at 240 nm. Ash content (wt%) was determined by oxidation of the remaining solid residue in a muffle furnace (4–10, Yongguangming instrument factory, Beijing) at 575 °C for 24 h while acid-insoluble lignin fraction (wt%) was obtained by the difference of weight loss. The analysis was parallelly performed twice (Table 1).

Other characterized methods for biomass. XRD, SEM and FT-IR analyses were also performed for biomass similar for catalysts in above section. The degree of crystallinity (*CrI*) in biomass was calculated as the ratio of cellulose I in mixed crystalline structure from XRD data²⁶:

$$CrI (\%) = (I_{002} - I_{am}) / I_{002} \times 100\% \quad (1)$$

Catalyst number	Weight ratio of glucose/Fe ₃ O ₄	Carbonization temperature (°C)	Carbonization time (h)	Sulfonation time (h) at 150 °C
1	6	650	0.5	19
2	6	700	1	20
3	6	750	1.5	21
4	7.5	650	1	21
5	7.5	700	1.5	19
6	7.5	750	0.5	20
7	9	650	1.5	20
8	9	700	0.5	21
9	9	750	1	19
10	6	700	1	19

Table 2. Orthogonal design for catalysts synthesized under different conditions.

where I_{002} is the peak intensity at diffraction angle $2\theta = 22^\circ$, whereas I_{am} is the height for the amorphous cellulose at $2\theta = 18^\circ$.

Hydrolysate analyses. After hydrolysis, the aqueous solution was filtrated with a 0.22 μm filter for total organic carbon (TOC-VCPN; FA, CN200, Shimadzu), UV-Vis and HPLC (LC-20A, Shimadzu) analyses. In TOC analysis, standard glucose aqueous solution with four carbon concentrations (250, 500, 750 and 1000 mg/mL) was used to calibrate the curve ($R^2 = 0.9985$). The concentration of total reducing sugars (TRS) in hydrolysate was determined using DNS (3,5-dinitrosalicylic acid) method with glucose as standard sample²⁷. The absorbance of aqueous solution was measured at 540 nm using UV-Vis spectrometer, and TRS was quantified by external standard curve method with five glucose concentration (0.1, 0.2, 0.3, 0.4 and 0.5 mg/mL; $R^2 = 0.9987$). Products (glucose, xylose, formic acid, acetic acid, HMF and furfural) in aqueous phase were also analyzed by HPLC equipped with an HPX-87H column, UV and refractive index detector, and calibrated with five standard points (0.1, 0.2, 0.4, 0.8 and 1.6 mg/mL, $R^2 = 0.9999$). Sulfuric acid aqueous solution (0.01 mmol L⁻¹) was used as mobile phase at flow rate of 0.6 mL min⁻¹, and column temperature was 60 °C.

Product yields and selectivities (wt%) were defined as follows:

$$\text{Glucose yield (wt\%)} = (\text{glucose weight in hydrolysate}) / (\text{glucose weight in raw material}) \times 100\% \quad (2)$$

$$\text{Xylose yield (wt\%)} = (\text{xylose weight in hydrolysate}) / (\text{xylose weight in raw material}) \times 100\% \quad (3)$$

$$\text{TRS yield (wt\%)} = (\text{TRS weight in hydrolysate}) / [\text{total weight of (glucose + xylose + mannose + arabinose) in raw material}] \times 100\% \quad (4)$$

$$\begin{aligned} \text{Product (glucose, formic acid, acetic acid, HMF, furfural) selectivity (wt\%)} \\ = \text{product carbon weight} / \text{TOC in hydrolysate} \times 100\% \end{aligned} \quad (5)$$

Results and Discussion

Component analyses of the three tropical biomass wastes (*bagasse*, *Jatropha* and *Plukenetia* hulls) are summarized in Table 1. Magnetic catalysts were synthesized under different conditions according to an orthogonal design (Table 2), and their activities tested by cellulose hydrolysis are listed in Table 3. Photos for the tropical plant wastes and catalyst separation by a magnet after reaction are demonstrated in Fig. 1. XRD, VSM, NH₃-TPD, FT-IR and SEM photos of the magnetic catalyst before and after sulfonation are presented in Figs 2–6, respectively. XRD, FT-IR and SEM photos of ball-milled cellulose, original tropical plant wastes before and after reaction are illustrated in Figs 7–10, respectively. The screened magnetic catalyst is used for the single-factor optimization of cellulose hydrolysis with TRS and glucose yields illustrated in Fig. 11. Catalyst cycles for milled-cellulose hydrolysis is displayed in Fig. 12. The assignment of major IR absorptions of magnetic catalyst (before and after sulfonation) and biomass wastes (before and after reactions) was illustrated in Tables 4 and 5, respectively. The hydrolysis results for original, ball-milled, water-extracted, water and ethanol extracted tropical plant wastes are given in Table 6.

Catalyst number	N (%)	C (%)	H (%)	S (%)	Acid density by S content (mmol g ⁻¹)	TRS yield (%) ^a	Glucose yield (%) ^a	Glucose selectivity (%) ^a
1	0.061	55.50	2.00	1.15	0.36	17.1 ± 1.4	9.1 ± 2.4	39.6 ± 2.4
2	0.052	58.00	1.82	1.02	0.32	17.7 ± 1.6	10.2 ± 0.4	41.6 ± 2.8
3	0.058	53.87	1.99	1.11	0.35	17.1 ± 0.5	8.0 ± 2.1	37.5 ± 1.6
4	0.061	55.50	2.00	1.15	0.36	17.2 ± 0.5	9.6 ± 2.3	41.8 ± 2.8
5	0.066	56.53	2.04	1.08	0.34	17.5 ± 1.7	9.2 ± 1.9	39.5 ± 1.5
6	0.039	60.91	2.01	0.91	0.28	16.9 ± 1.9	8.9 ± 0.4	40.5 ± 2.5
7	0.063	59.98	2.17	1.00	0.31	14.8 ± 2.4	7.2 ± 0.7	36.2 ± 0.3
8	0.060	61.79	2.10	0.97	0.30	17.7 ± 3.1	8.1 ± 0.8	36.8 ± 1.9
9	0.060	61.62	2.13	0.95	0.30	13.5 ± 2.9	6.1 ± 1.3	34.3 ± 0.8
10	0.034	53.00	2.10	1.28	0.40	18.5 ± 1.5	10.3 ± 2.1	41.4 ± 3.2

Table 3. Activity of catalysts synthesized under different conditions for ball-milled cellulose hydrolysis.

^aConditions for hydrolysis reactions: ball-milled cellulose 0.027 g, catalyst 0.15 g, water 15 mL, 180 °C for 3 h. Two repetitions were done for each run.

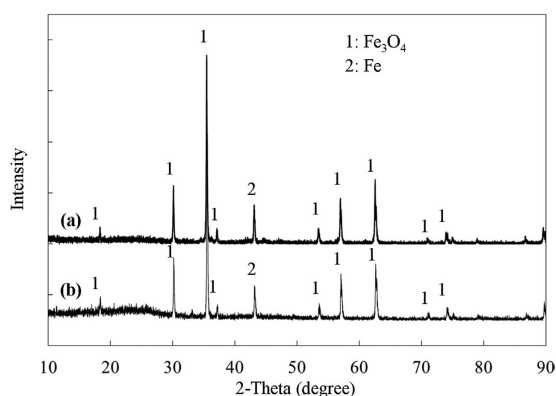


Figure 2. XRD patterns of the screened magnetic catalyst: (a) before sulfonation (C/Fe₃O₄) and (b) after sulfonation (C-SO₃H/Fe₃O₄).

Catalyst screening. Catalysts were prepared according to an orthogonal design [Table 2, L9(3⁴)] with four factors: weight ratio of glucose/Fe₃O₄ (6, 7.5, 9), carbonization temperature (650, 700, 750 °C), carbonization time (0.5, 1, 1.5 h) and sulfonation time (19, 20, 21 h). The optimized conditions for catalyst synthesis were glucose/Fe₃O₄ weight ratio of 6/1, carbonization temperature of 700 °C, carbonization time of 1 h and sulfonation time of 19 h, with the highest acid density of 0.40 mmol g⁻¹ being achieved for the catalyst (Table 3; No# 10). In the presence of the optimized No# 10 catalyst (denoted as C-SO₃H/Fe₃O₄), ball-milled cellulose was hydrolyzed at 180 °C for 3 h²⁸, giving the highest TRS and glucose yields of 18.5% and 10.3%, respectively with hydrolysis yield [total organic carbon (TOC) in hydrolysate/carbon weight in cellulose × 100%] of 41.4%, that was slightly lower to the value (48.6%) over the magnetic catalyst (Fe₃O₄@C-SO₃H) in previous work at 140 °C for 12 h¹⁶. The screened magnetic catalyst was further characterized and used for biomass hydrolysis below.

Catalyst characterization. Figure 2 illustrated the crystalline structures of the catalyst before and after sulfonation (C/Fe₃O₄ vs. C-SO₃H/Fe₃O₄). According to Joint Committee on Powder Diffraction Standard (JCPDS card No. 19–629), XRD peaks were identified as crystalline phases of Fe₃O₄ and Fe. Some of Fe₃O₄ was reduced to Fe by carbon in the pyrolysis process at 700 °C. There was no carbon peak detected, indicating carbon was in amorphous phase. During sulfonation, Fe₃O₄/Fe encapsulated in the carbon shell of catalyst converted little to iron sulphate by concentrated H₂SO₄, protected from the amorphous carbon¹⁵. However, some Fe₃O₄ particles remained on the surface after pyrolysis were converted to iron sulphate that was totally removed by washing several times with distilled water in the 50 mL autoclave at 200 °C for 3 h (detected using CaCl₂). After sulfonation, no significant difference was seen in the crystalline phases between C/Fe₃O₄ and C-SO₃H/Fe₃O₄.

Magnetic saturation (Ms) of the catalyst was 26.35, 19.5 and 12.9 Am² kg⁻¹ before sulfonation, after sulfonation, and after seven cycles for cellulose hydrolysis, respectively (Fig. 3). The decline in catalyst magnetism was due to the leaching of Fe₃O₄ by concentrated H₂SO₄ in sulfonation and residue

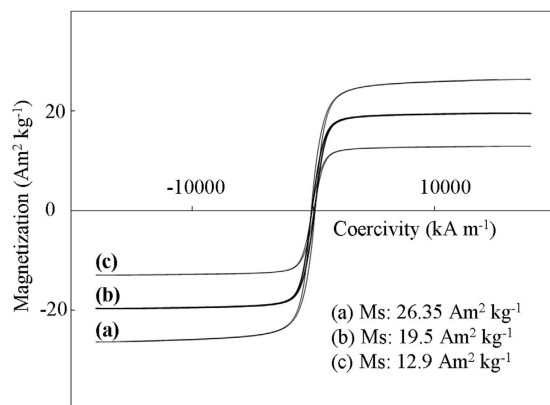


Figure 3. VSM curves for magnetic catalyst: (a) before sulfonation (C/Fe_3O_4), (b) after sulfonation ($C-SO_3H/Fe_3O_4$), and (c) after seven cycles ($C-SO_3H/Fe_3O_4$).

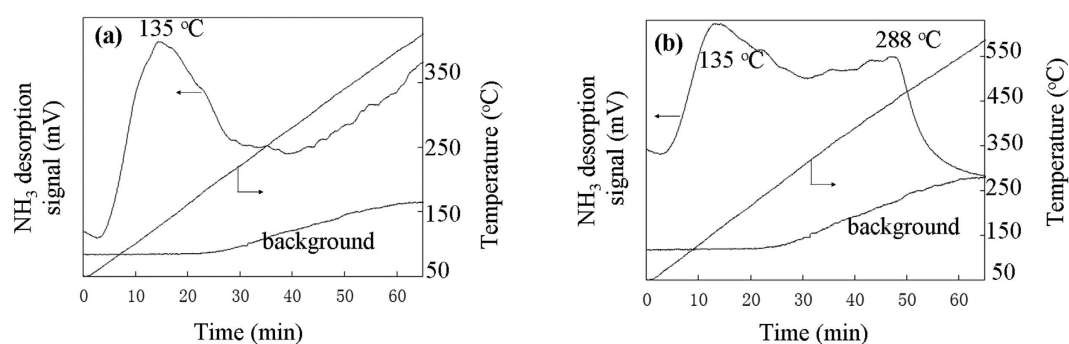


Figure 4. NH_3 -TPD curves of magnetic carbonaceous acid: (a) before sulfonation (C/Fe_3O_4 , acidity of 0.17 mmol g^{-1}) and (b) after sulfonation ($C-SO_3H/Fe_3O_4$, acidity of 0.96 mmol g^{-1}) (background without NH_3).

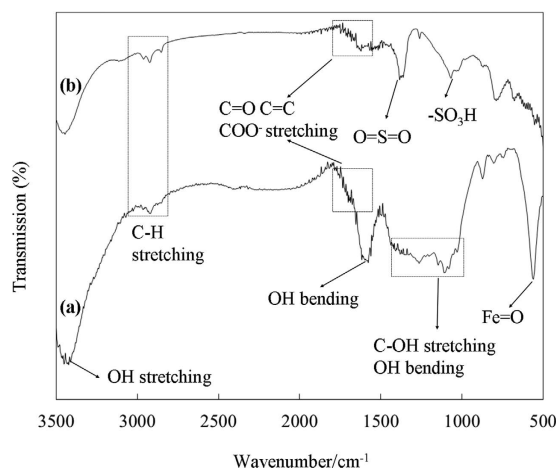


Figure 5. FT-IR spectra of magnetic catalyst: (a) before sulfonation (C/Fe_3O_4) and (b) after sulfonation ($C-SO_3H/Fe_3O_4$).

deposition on the surface of catalyst during the cycles. The M_s value is comparable with that ($23 \text{ Am}^2 \text{ kg}^{-1}$) reported in literature¹⁶.

In Fig. 4, the catalyst (before and after sulfonation) showed a major desorption peak at $135 \text{ }^\circ\text{C}$, because of the weak acid sites ($-OH$ and $-COOH$) of incompletely formed carbon sheets²⁹. After sulfonation, catalyst $C-SO_3H/Fe_3O_4$ had a strong peak at $288 \text{ }^\circ\text{C}$ from $-SO_3H$ group with total acid density (mmol g^{-1})

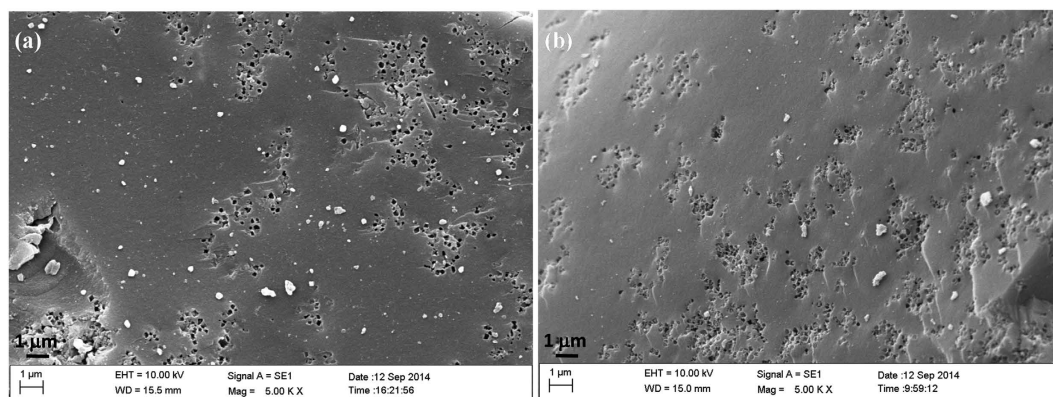


Figure 6. SEM images of magnetic catalyst: (a) before sulfonation (C/Fe_3O_4) and (b) after sulfonation ($C-SO_3H/Fe_3O_4$).

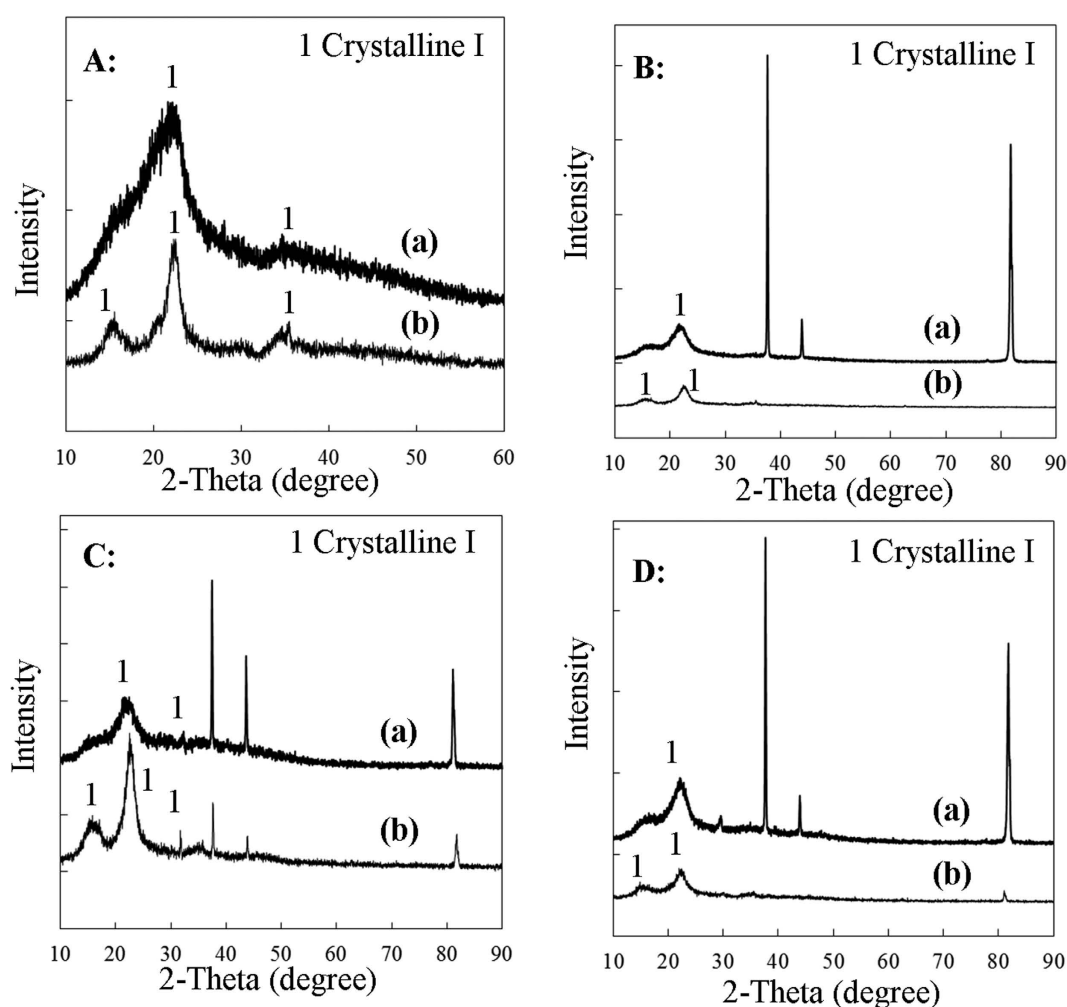


Figure 7. XRD patterns of original biomass materials: (A) ball-milled cellulose, (B) original bagasse, (C) original *Jatropha* hulls, and (D) original *Plukenetia* hulls (a: before reaction and b: after reaction).

increased to 0.96 (vs. 0.17 for C/Fe_3O_4) as compared to 0.40 by elemental analysis and 0.75 by NaOH titration.

In Fig. 5, absorption at 566 cm^{-1} was from the Fe-O vibration in Fe_3O_4 ³⁰, $1600\text{--}1800\text{ cm}^{-1}$ were from COO^- , C=O and C=C stretching vibrations³¹, and 3463 cm^{-1} was from -OH stretching vibration with its hydrophilic surface for easier contact between reactant and catalyst³². After sulfonation, two bands at

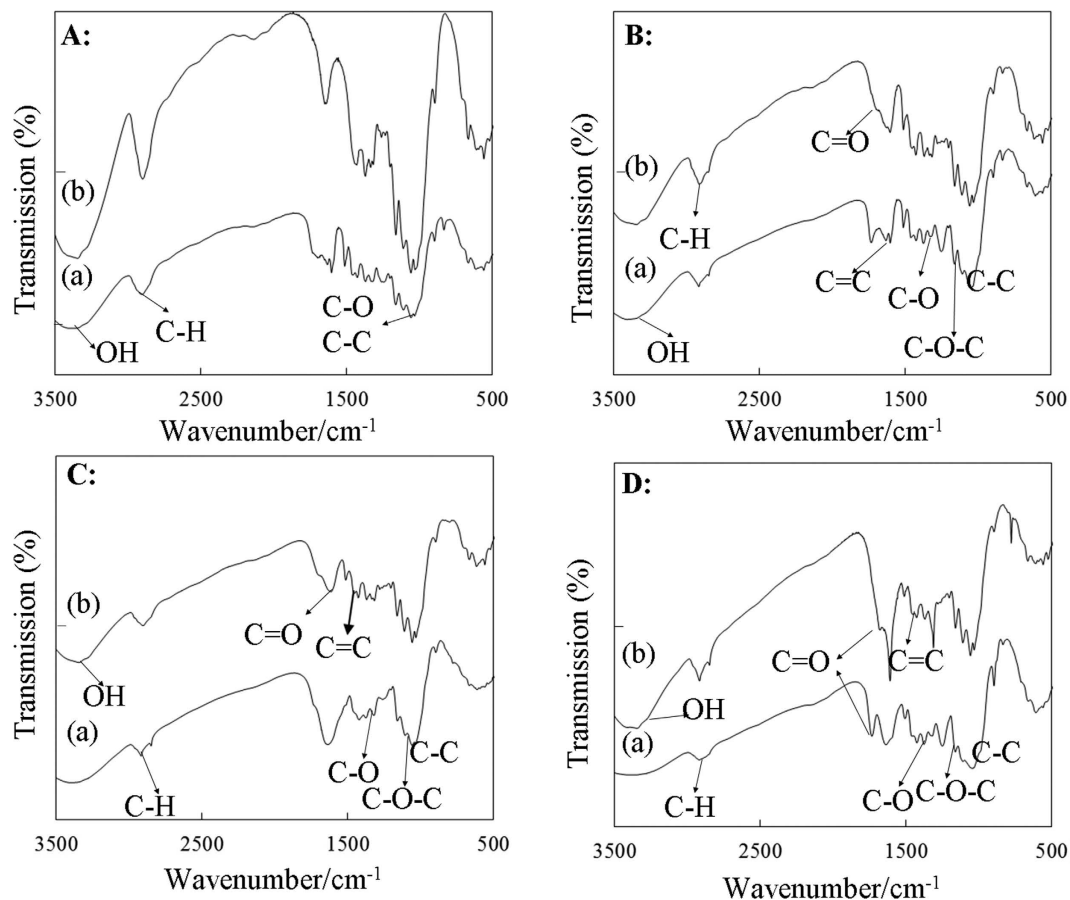


Figure 8. FT-IR spectra of biomass: (A) ball-milled cellulose, (B) original bagasse, (D) original *Jatropha* hulls, and (D) original *Plukenetia* hulls (a: before reaction and b: after reaction).

1066 ($-\text{SO}_3^-$ stretching) and 1363 cm^{-1} ($\text{O}=\text{S}=\text{O}$ stretching in $-\text{SO}_3\text{H}$) appeared because the catalyst was functionalized with $-\text{SO}_3\text{H}$ group (Fig. 5b and Table 4).

SEM images (Fig. 6) showed the catalyst changed little after sulfonation, both particles had smooth surfaces with numerous pores on the surfaces.

Biomass characterization. XRD results of four biomass materials before and after hydrolysis are given in Fig. 7. Ball-milled cellulose had a strong peak at angle (2θ) of about 22° , corresponding to crystalline cellulose I. the degree of crystallinity was only 41% calculated by equation (1). After hydrolysis, three crystalline peaks at angle (2θ) of about 16° , 22° , and 35° became apparent, which were identified as the lattice plane ($10\bar{1}$), (002) and (040) of crystalline cellulose I, respectively²⁶. So, the degree of crystallinity of cellulose after hydrolysis increased to 69%. The hydrogen-bonding structure of amorphous cellulose was much weaker than that of cellulose I, which made the amorphous part in ball-milled cellulose easier degraded in hydrolysis reaction, and left only crystalline cellulose I. Similar phenomenon was also observed for original bagasse, *Jatropha* and *Plukenetia* hulls (Fig. 7b–d) with the degree of cellulose crystallinity rose from 46%, 42% and 54% before hydrolysis to 78%, 72% and 60% after hydrolysis, respectively.

For ball-milled cellulose, absorptions at about 2880 and $3000\text{--}3500\text{ cm}^{-1}$ were due to C-H and -OH stretching, respectively, while absorption at $950\text{--}1200\text{ cm}^{-1}$ was from C-O/C-C stretching or C-H bending (Fig. 8 and Table 5)³³. The original tropical plant wastes had an apparent characteristic absorption at 1155 cm^{-1} that was generally due to the C-O-C asymmetric bridge stretching of glycans, as well as characteristic absorptions at 1725 cm^{-1} for C=O stretching, 1599 and 1509 cm^{-1} for C=C stretching in aromatic ring and 1263 cm^{-1} related to C(O)-O stretching³⁴. After hydrolysis, the main absorptions still existed, while the intensity of C-O stretching of glycans decreased, indicating the lignocellulosic structure remained although part of glycans were degraded (Fig. 8b–d).

The surface morphologies of ball-milled cellulose, original bagasse, *Jatropha* and *Plukenetia* hulls before and after reactions were observed by SEM (Figs 9 and 10). The four biomass samples showed a relatively compact and rigid surface before hydrolysis, but after reaction they exhibited a corrugated and more porous surface, revealing the disruption of tissue network and the destruction of highly ordered structure.

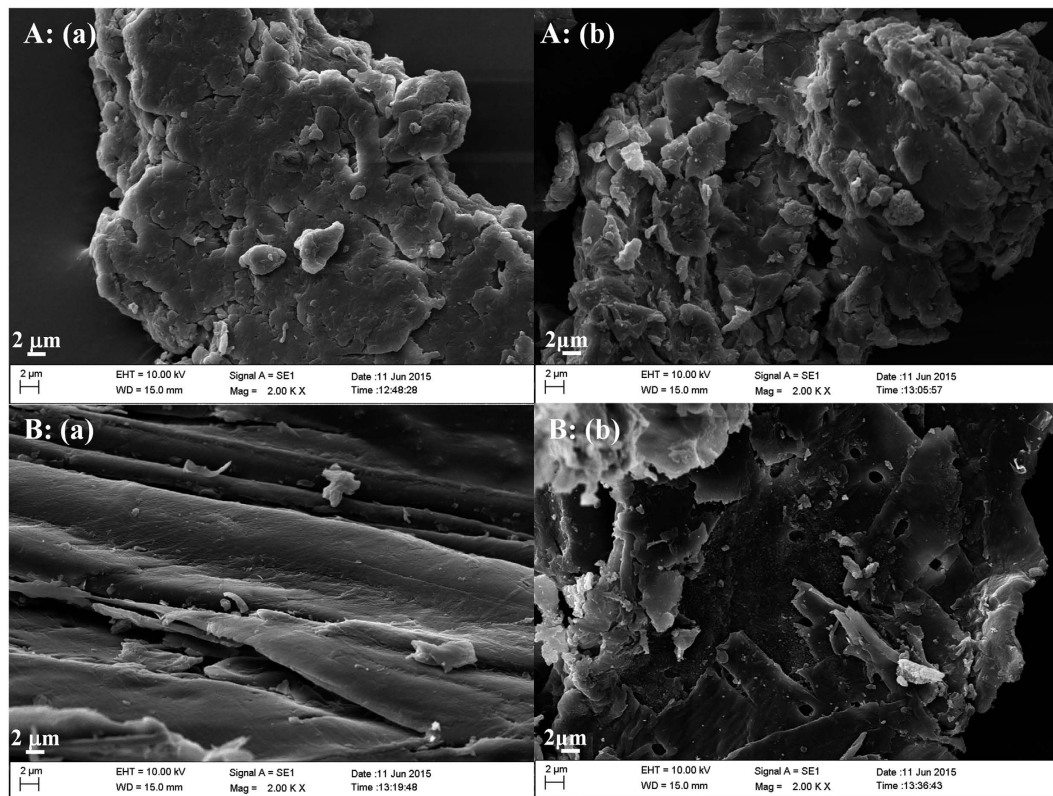


Figure 9. SEM images of (A) ball-milled cellulose and (B) original bagasse (a: before reaction and b: after reaction).

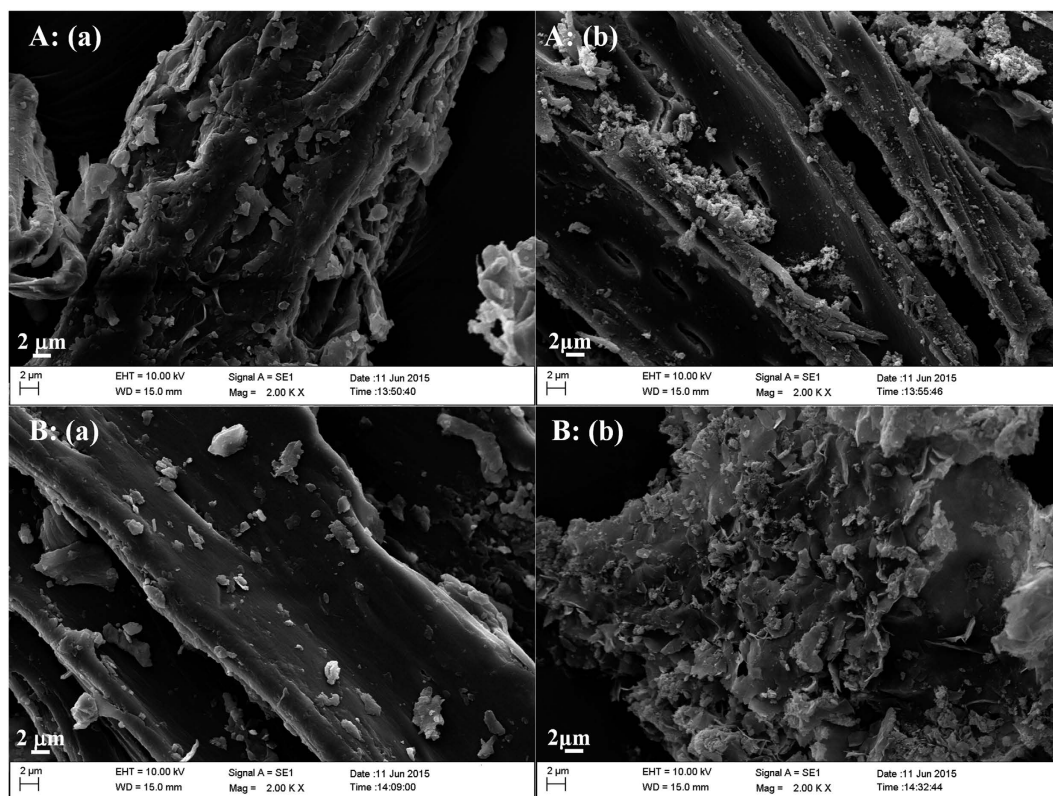


Figure 10. SEM images of (A) original *Jatropa* hulls and (B) original *Plukenetia* hulls (a: before reaction and b: after reaction).

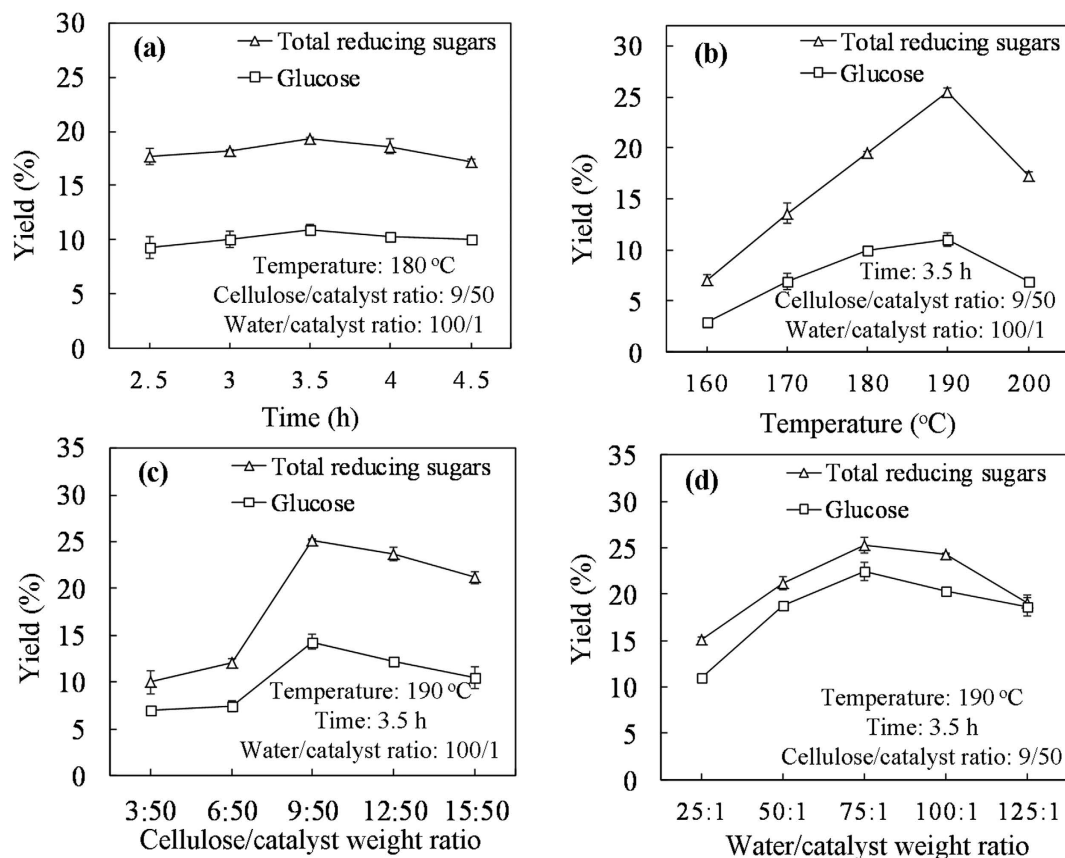


Figure 11. Single-factor test of ball-milled cellulose hydrolysis with C-SO₃H/Fe₃O₄ catalyst: (a) time, (b) temperature, (c) cellulose/catalyst weight ratio, and (d) water/catalyst weight ratio.

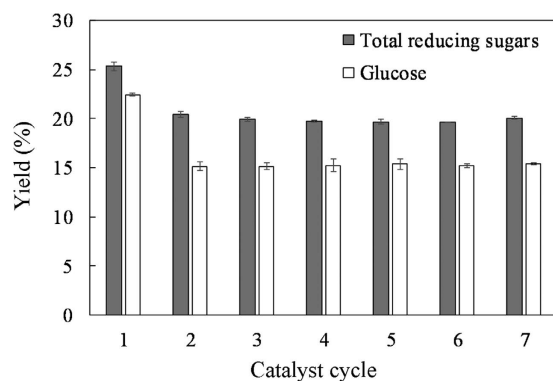


Figure 12. C-SO₃H/Fe₃O₄ catalyst cycle for ball-milled cellulose hydrolysis.

Cellulose hydrolysis. Single-factor optimization. Referred to previous studies^{12,35}, four factors including reaction time (2.5–4.5 h, excluding initial heating and final cooling times), reaction temperature (160–200 °C), cellulose/catalyst weight ratio (3/50–15/50) and water/catalyst weight ratio (25/1–125/1) were optimized for ball-milled cellulose hydrolysis by single-factor test, and the results were plotted in Fig. 11.

Reaction time. Under the fixed conditions (180 °C, cellulose/catalyst weight ratio of 9/50 and water/cellulose weight ratio of 100/1), the influence of reaction time was studied (Fig. 11a). Cellulose was first hydrolyzed to sugars and further degraded to small organic substances such as HMF, levulinic acid and formic acid¹⁴. As time increased from 2.5 to 3.5 h, TRS and glucose yields rose from 17.7% and 9.3% to 19.3% and 10.9%, respectively with minor byproducts levulinic acid (4.3%) and formic acid (2.1%), and

Major absorptions	Wavenumber (cm ⁻¹)	
	C/Fe ₃ O ₄ (Fig. 5a)	C-SO ₃ H/Fe ₃ O ₄ (Fig. 5b)
Fe=O stretching	566	538
-SO ₃ ⁻ stretching	–	1066
O=S=O stretching	–	1363
OH bending	1686	1636
C=O, C=C, COO ⁻ stretching	1600–1800	1600–1800
C-H stretching	2863–3075	2863–3075
OH stretching	3463	3438

Table 4. Major IR absorptions of magnetic catalyst before and after sulfonation (Fig. 5)^{30–32}.

Major absorptions	Wavenumber (cm ⁻¹)							
	Cellulose (Fig. 8A)		Bagasse (Fig. 8B)		Jatropha hulls (Fig. 8C)		Jatropha hulls (Fig. 8D)	
	Before hydrolysis	After hydrolysis	Before hydrolysis	After hydrolysis	Before hydrolysis	After hydrolysis	Before hydrolysis	After hydrolysis
C-C stretching	1036	1045	950–1200	950–1200	950–1200	950–1200	950–1200	950–1200
C-O-C stretching	–	–	1155	1128	1086	1032	1123	1076
C-O stretching	1256	1260	1263	1203	1203	1163	1236	1176
C=C stretching	–	–	1599	1518	1508	1558	1575	1535
C=O stretching	–	–	1725	1683	1686	1657	1701	1635
C-H stretching	2882	2878	2880	2826	2763	2704	2781	2808
-OH stretching	3463	3446	3463	3369	3456	3218	3438	3357

Table 5. Major IR absorptions of biomass wastes before and after reactions (Fig. 8)^{33,34}.

slight HMF at 3.5 h. After 3.5 h, both TRS and glucose yields slightly decreased. Reaction time of 3.5 h was selected as the best value.

Reaction temperature. Reaction temperature from 160 to 200 °C was used to hydrolyze cellulose under the conditions (reaction time of 3.5 h, cellulose/catalyst weight ratio of 9/50 and water/cellulose weight ratio of 100/1) (Fig. 11b). At 160 °C, TRS (7.1%) and glucose yields (2.9%) were quite low. At 190 °C, the yields of TRS and glucose jumped sharply to 25.6% and 11.0%, respectively. However, at temperature >190 °C, they dropped remarkably owing to the decomposition to HMF and levulinic acid with the yields of 5.8% and 6.4%, respectively. The yields of levulinic acid and formic acid reached their high levels of 6.5% and 3.2%, respectively at 180 °C. Reaction temperature of 190 °C was selected for the following experiments.

Cellulose/catalyst weight ratio. Cellulose/catalyst weight ratio varied from 3/50 to 15/50 for cellulose hydrolysis with reaction time of 3.5 h, temperature of 190 °C and water/catalyst weight ratio of 100/1. In the absence of catalyst, only 3.4% TRS and 1.8% glucose yields were produced. In Fig. 11c, after catalyst (0.05 g) was added to the reaction system (cellulose/catalyst weight ratio of 3/50), 10.0% TRS and 7.0% glucose yields were obtained. The yields of TRS and glucose grew to 25.2% and 14.3%, respectively at higher cellulose/catalyst weight ratio of 9/50. However, as the weight ratio increased further from 9/50 to 15/50, TRS and glucose yields reduced slightly to 21.2% and 10.5%, respectively because of the enhancement of byproducts such as HMF (5.1%), acetic acid (3.2%) and formic acid (3.6%). So, cellulose/catalyst weight ratio of 9/50 was chosen as the best value. In previous literatures^{11,12,16}, catalyst/cellulose weight ratio for cellulose hydrolysis was normally high (e.g., 1/1¹¹, 12/1¹² 3/1¹⁶ vs. 5.6/1 in this work) because of the weak acidity and heterogeneous reaction condition. However, considering the economic sustainability, the amount of solid catalyst should be limited. Decreasing the crystallinity of cellulosic materials by pretreatment, improving the activity of solid catalysts and enhancing the mixture of reactants (e.g., by ultrasound) may be the possible methods to achieve the purpose.

Water/catalyst weight ratio. Water/catalyst weight ratio was changed from 25/1 to 125/1 under the conditions of reaction time of 3.5 h, temperature of 190 °C and cellulose/catalyst weight ratio of 9/50 for cellulose hydrolysis (Fig. 11d). TRS and glucose yields increased from 15.1% and 11.0% to 25.3% and

Biomass	Yield (%)			Product selectivity (%)				
	TRS	Glucose	Xylose	Glucose	Formic acid	Acetic acid	HMF	Furfural
Bagasse								
original	57.0 ± 1.8	42.6 ± 3.5	95.7 ± 1.9	60.1 ± 1.4	1.2 ± 0.9	6.0 ± 1.6	3.1 ± 0.3	5.6 ± 1.2
ball-milled	68.4 ± 1.2	51.1 ± 1.4	96.1 ± 1.2	71.1 ± 0.7	1.8 ± 0.5	4.7 ± 3.1	5.2 ± 2.4	6.3 ± 2.5
water-extracted	71.3 ± 0.9	54.1 ± 3.1	94.7 ± 2.1	77.4 ± 1.7	1.9 ± 1.2	5.1 ± 1.6	4.9 ± 1.4	5.8 ± 2.7
water-ethanol extracted	79.8 ± 1.2	58.3 ± 2.1	97.2 ± 1.6	82.2 ± 3.1	2.3 ± 3.2	4.6 ± 3.2	5.0 ± 3.0	4.9 ± 1.6
<i>Jatropha</i> hulls								
original	29.5 ± 2.1	22.2 ± 2.5	95.3 ± 3.2	46.7 ± 2.0	6.9 ± 1.6	2.7 ± 0.8	0.2 ± 0.2	0.0
ball-milled	35.4 ± 3.1	26.7 ± 0.4	95.6 ± 2.1	56.0 ± 3.1	6.2 ± 0.4	2.4 ± 1.4	1.4 ± 0.2	0.8 ± 1.8
water-extracted	41.2 ± 1.5	31.1 ± 1.3	94.8 ± 1.0	63.4 ± 1.5	5.9 ± 1.1	2.6 ± 1.1	1.6 ± 1.1	1.2 ± 0.7
water-ethanol extracted	47.2 ± 0.6	35.6 ± 1.9	96.4 ± 2.6	70.1 ± 0.4	6.0 ± 0.9	3.1 ± 0.6	2.3 ± 0.1	0.9 ± 0.2
<i>Plukenetia</i> hulls								
original	34.0 ± 2.2	20.5 ± 1.6	97.9 ± 2.6	42.8 ± 0.7	5.1 ± 0.8	8.3 ± 1.1	0.5 ± 0.4	3.1 ± 0.7
ball-milled	40.8 ± 1.4	24.6 ± 1.2	96.8 ± 0.3	50.4 ± 3.0	4.9 ± 2.5	7.6 ± 1.7	1.3 ± 0.9	3.4 ± 1.7
water-extracted	44.2 ± 1.2	28.7 ± 0.6	95.7 ± 1.3	58.9 ± 0.3	3.8 ± 1.1	6.2 ± 0.7	1.5 ± 1.3	2.8 ± 1.1
water-ethanol extracted	54.4 ± 0.4	35.8 ± 1.3	94.9 ± 0.9	68.5 ± 1.5	4.5 ± 0.5	7.4 ± 0.7	1.5 ± 1.1	3.5 ± 0.9

Table 6. Hydrolysis of the three tropical biomass wastes^a. ^aConditions for hydrolysis reactions: biomass 0.027 g, catalyst 0.15 g, water 11.25 mL, 190 °C for 3.5 h. Two repetitions were done for each run.

22.4%, respectively as water/catalyst weight ratio grew from 25/1 to 75/1, meanwhile, glucose selectivity reached 45.0%. As the weight ratio rose further from 75/1 to 125/1, TRS and glucose yields declined to 19.1% and 18.7%, respectively because of the leaching or deactivation of the active sites of catalyst by excess water³⁰. Therefore, the best value for water/catalyst weight ratio was 75/1.

In conclusion, the selected best conditions for ball-milled cellulose hydrolysis with glucose yield of 22.4%, TRS yield of 25.3% and glucose selectivity of 48% were as follows: reaction time of 3.5 h, reaction temperature of 190 °C, cellulose/catalyst weight ratio of 9/50 and water/catalyst weight ratio of 75/1. The above conditions were used in the following experiments for catalyst cycles and hydrolysis of the tropical biomass wastes.

Catalyst cycles. Under the above best conditions, C-SO₃H/Fe₃O₄ catalyst was conducted recycle experiments for ball-milled cellulose hydrolysis (Fig. 12). The recovery rate of catalyst was 92.8% after seven cycles. In the second cycle, TRS and glucose yields decreased from 25.3% and 22.4% to 20.5% and 15.1%, respectively. Correspondingly, the total acid density of the catalyst decreased from 0.96 to 0.83 mmol g⁻¹ after one cycle by NH₃-TPD analysis. However, both TRS and glucose yields changed little after the second cycle (20.1% TRS and 15.4% glucose yields at the seventh cycle), indicating good stability of the second cycled catalyst. NH₃-TPD analysis also showed the relative stable acid density (0.83 and 0.70 mmol g⁻¹ after the first and seventh cycles). On the other hand, the total acid density was 0.75 for fresh catalyst and 0.63 mmol g⁻¹ after seven cycles by NaOH titration.

In conclusion, C-SO₃H/Fe₃O₄ catalyst can cycle at least seven times with relatively high TRS yield of 20.1%, glucose yield of 15.4% and catalyst recovery of 92.8% at the seventh cycle.

Hydrolysis of tropical biomass wastes. Under the best conditions obtained for cellulose, the catalyst was applied to the hydrolysis of original, ball-milled, water-extracted, water and ethanol extracted tropical plant wastes: bagasse, *Jatropha* and *Plukenetia* hulls (Table 6). Every experiment was conducted in duplicate.

For original bagasse hydrolysis, 57.0% TRS, 42.6% glucose and 95.7% xylose yields were obtained at 190 °C for 3.5 h that were much higher than those yields from ball-milled cellulose. It demonstrated that the interpolation and bonding of hemicellulose with cellulose in native plants destroyed the rigorous and recalcitrant structure of pure cellulose to benefit the degradation of cellulose part⁴. However, the degradation of monosaccharides to byproducts such as acetic acid, furfural and HMF was also promoted with the yields of 6.0%, 5.6% and 3.1%, respectively.

Compared with bagasse, the glucan and xylan contents of *Jatropha* and *Plukenetia* hulls were lower (34.1% and 30.5% vs. 40.1%; 10.3% and 15.1% vs. 18.5%, Table 1). The remarkable difference of *Jatropha* and *Plukenetia* hulls from bagasse was that the hulls contain higher extractives (16.8% and 17.6% vs. 9.8%), such as fatty oils and phenols (identified before for *Jatropha* hulls³⁶). These extractives cannot be hydrolyzed and bonded to glucan to prevent it contact with water molecules and catalyst for hydrolysis. *Jatropha* and *Plukenetia* hulls had low TRS yields of 29.5% and 34.0% (vs. 57.0% for bagasse), respectively.

Glucose yield was also reduced sharply from 42.6% for bagasse to 22.2% and 20.5% for *Jatropha* and *Plukenetia* hulls, while xylose yield still kept high with little change due to the easy hydrolysis for xylan.

Pretreatments of the tropical biomass samples by ball-milling, water extraction, water-ethanol extraction were conducted to destroy biomass structure or remove extractives to improve the production of TRS and glucose. After ball-milled, TRS and glucose yields of 68.4% and 51.1% for bagasse, 35.4% and 26.7% for *Jatropha* hulls, as well as 40.8% and 24.6% for *Plukenetia* hulls were obtained, which was attributed to easier hydrolysis because of the structural damage of crystalline cellulose and extractives. For water-ethanol extracted bagasse, *Jatropha* and *Plukenetia* hulls, TRS and glucose yields increased to 79.8% and 58.3% (vs. 57% and 42.6%), 47.2% and 35.6% (vs. 29.5% and 22.2%), 54.4% and 35.8% (vs. 34% and 20.5%), respectively compared with original materials, which could be due to the removal of extractable composition in raw biomass that hindered biomass hydrolysis and catalyst activity. Meanwhile, the formation of by-products such as furfurals and small organic acids in biomass hydrolysis had no significant changes, which made the product selectivity of glucose from cellulose remarkably increased after pretreatment.

It can be concluded that the catalyst showed a better activity in the hydrolysis of bagasse. For original bagasse, *Jatropha* and *Plukenetia* hulls, proper treatment such as ball-milling and solvent extraction improved hydrolysis yields significantly.

Conclusions

Catalyst C-SO₃H/Fe₃O₄ with strong magnetism (19.5 Am² kg⁻¹) and high total acid density (0.75 mmol g⁻¹, NaOH titration) was synthesized and screened for the hydrolysis of cellulose and tropical plant wastes in microwave reactor. It was cycled seven times with little deactivation and magnetism loss. The best hydrolysis conditions for ball-milled cellulose were optimized with single-factor optimization with the yields of reducing sugars and glucose of 25.3% and 22.4%, respectively. The catalyst was used to hydrolyze bagasse, *Jatropha* and *Plukenetia* hulls with the highest glucose yield of 58.3%, 35.6% and 35.8%, respectively. Pretreatment of tropical biomass greatly improved hydrolysis yield and glucose selectivity.

References

- National Development and Reform Commission of China. Development planning of sugarcane in main production areas from 2015 to 2020. Document # 1101(2015). in Chinese.
- Yang, C. Y., Fang, Z., Li, B. & Long, Y. F. Review and prospects of *Jatropha* biodiesel industry in China. *Renewable Sustainable Energy Rev.* **16**, 2178–2190 (2012).
- Liu, Q. *et al.* Chemical composition and oxidative evolution of Sacha Inchi (*Plukenetia volubilis* L.) oil from Xishuangbanna (China). *Grasas Aceites* **65**, e012 (2014).
- Lai, D. M., Deng, L., Guo, Q. X. & Fu, Y. Hydrolysis of biomass by magnetic solid acid. *Energy Environ. Sci.* **4**, 3552–3557 (2011).
- Yu, Z. Y., Jameel, H., Chang, H. M., Philips, R. & Park, S. Quantification of bound and free enzymes during enzymatic hydrolysis and their reactivities on cellulose and lignocellulose. *Bioresour. Technol.* **147**, 369–377 (2013).
- Behera, S., Arora, R., Nandhagopal, N. & Kumar, S. Importance of chemical pretreatment for bioconversion of lignocellulosic biomass. *Renewable Sustainable Energy Rev.* **36**, 91–106 (2014).
- Besson, M., Gallezot, P. & Pinel, C. Conversion of biomass into chemicals over metal catalysts. *Chem. Rev.* **114**, 1827–1870 (2014).
- Margolese, D., Melero, J. A., Christiansen, S. C., Chmelka, B. F. & Stucky, G. D. Direct syntheses of ordered SBA-15 mesoporous silica containing sulfonic acid groups. *Chem. Mater.* **12**, 2448–2459 (2000).
- Agirrezabal-Telleria, I., Hemmann, F., Jäger, C., Arias, P. L. & Kemnitz, E. Functionalized partially hydroxylated MgF₂ as catalysts for the dehydration of d-xylose to furfural. *J. Catal.* **305**, 81–91 (2013).
- Anderson, J. M., Johnson, R. L., Schmidt-Rohr, K. & Shanks, B. H. Solid state NMR study of chemical structure and hydrothermal deactivation of moderate-temperature carbon materials with acidic SO₃H sites. *Carbon* **74**, 333–345 (2014).
- Pang, J. F., Wang, A. Q., Zheng, M. Y. & Zhang, T. Hydrolysis of cellulose into glucose over carbons sulfonated at elevated temperatures. *Chem. Commun.* **46**, 6935–6937 (2010).
- Suganuma, S. *et al.* Hydrolysis of cellulose by amorphous carbon bearing SO₃H, COOH, and OH groups. *J. Am. Chem. Soc.* **130**, 12787–12793 (2008).
- Gill, C. S., Price, B. A. & Jones, C. W. Sulfonic acid-functionalized silica-coated magnetic nanoparticle catalysts. *J. Catal.* **251**, 145–152 (2007).
- Xiong, Y., Zhang, Z. H., Wang, X., Liu, B. & Lin, J. T. Hydrolysis of cellulose in ionic liquids catalyzed by a magnetically-recoverable solid acid catalyst. *Chem. Eng. J.* **235**, 349–355 (2014).
- Liu, W. J., Tian, K., Jiang, H. & Yu, H. Q. Facile synthesis of highly efficient and recyclable magnetic solid acid from biomass waste. *Sci. Rep.* **3**, 2419 (2013).
- Zhang, C. B., Wang, H. Y., Liu, F. D., Wang, L. & He, H. Magnetic core-shell Fe₃O₄@C-SO₃H nanoparticle catalyst for hydrolysis of cellulose. *Cellulose* **20**, 127–134 (2013).
- Liao, Y. H. *et al.* Promoting hydrolytic hydrogenation of cellulose to sugar alcohols by mixed ball milling of cellulose and solid acid catalyst. *Energy Fuels* **28**, 5778–5784 (2014).
- Saha, B. C., Iten, L. B., Cotta, M. A. & Wu, Y. V. Dilute acid pretreatment, enzymatic saccharification and fermentation of wheat straw to ethanol. *Process Biochem.* **40**, 3693–3700 (2005).
- Xin, D. L., Jia, L. L., Zhao, C. J. & Zhang, J. H. Behavior of cellulose and xylan in aqueous ammonia pretreatment. *Appl. Biochem. Biotechnol.* **174**, 2626–2638 (2014).
- Grasvik, J., Winstrand, S., Normark, M., Jonsson, L. J. & Mikkola, J. P. Evaluation of four ionic liquids for pretreatment of lignocellulosic biomass. *BMC Biotech.* **14**, 34 (2014).
- Ha, S. H., Mai, N. L., An, G. & Koo, Y. M. Microwave-assisted pretreatment of cellulose in ionic liquid for accelerated enzymatic hydrolysis. *Bioresour. Technol.* **102**, 1214–1219 (2011).
- Mascotto, S. *et al.* Effect of microwave assisted and conventional thermal heating on the evolution of nanostructured inorganic-organic hybrid materials to binary ZrO₂-SiO₂ oxides. *J. Mater. Chem.* **17**, 4387–4399 (2007).

23. Boehm, H. P. Surface oxides on carbon and their analysis: A critical assessment. *Carbon* **40**, 145–149 (2002).
24. Fan, S. P. *et al.* High yield production of sugars from deproteinated palm kernel cake under microwave irradiation *via* dilute sulfuric acid hydrolysis. *Bioresour. Technol.* **153**, 69–78 (2014).
25. Sluiter, A., Hames, B., Ruiz, R., Scarlata, C. & Sluiter, B. Determination of structural carbohydrates and lignin in biomass. Document # NREL/TP-510-42618 (National renewable energy laboratory, Golden Colorado, 2008).
26. Segal, L., Creely, J. J., Martin, A. E. & Conrad, C. M. An empirical method for estimating the degree of crystallinity of native cellulose using the X-ray diffractometer. *Text. Res. J.* **29**, 786–794 (1959).
27. Miller, G. L. Use of dinitrosalicylic acid reagent for determination of reducing sugar. *Anal. Chem.* **31**, 426–428 (1959).
28. Huang, Y. B. & Fu, Y. Hydrolysis of cellulose to glucose by solid acid catalysts. *Green Chem.* **15**, 1095–1111 (2013).
29. Kanbur, Y. & Kucukyavuz, Z. Synthesis and characterization of surface modified fullerene. *Fullerenes Nanotubes Carbon Nanostruct.* **20**, 119–126 (2012).
30. Guo, H. X., Lian, Y. F., Yan, L. L., Qi, X. H. & Smith, R. L. Cellulose-derived superparamagnetic carbonaceous solid acid catalyst for cellulose hydrolysis in an ionic liquid or aqueous reaction system. *Green Chem.* **15**, 2167–2174 (2013).
31. Jiang, Y. J., Li, X. T., Cao, Q. & Mu, X. D. Acid functionalized, highly dispersed carbonaceous spheres: An effective solid acid for hydrolysis of polysaccharides. *J. Nanopart. Res.* **13**, 463–469 (2011).
32. Alvaro, M., Corma, A., Das, D., Fornés, V. & García, H. “Nafion”-functionalized mesoporous MCM-41 silica shows high activity and selectivity for carboxylic acid esterification and Friedel–Crafts acylation reactions. *J. Catal.* **231**, 48–55 (2005).
33. Yang, H. P., Yan, R., Chen, H. P., Lee, D. H. & Zheng, C. G. Characteristics of hemicellulose, cellulose and lignin pyrolysis. *Fuel* **86**, 1781–1788 (2007).
34. Trinh, L. T. P., Lee, Y. J., Lee, J. W. & Lee, H. J. Characterization of ionic liquid pretreatment and the bioconversion of pretreated mixed softwood biomass. *Biomass Bioenergy* **81**, 1–8 (2015).
35. Fukuhara, K. *et al.* Structure and catalysis of cellulose-derived amorphous carbon bearing SO₃H groups. *ChemSusChem* **4**, 778–784 (2011).
36. Jiang, L. Q., Fang, Z., Guo, F. & Yang, L. B. Production of 2,3-butanediol from acid hydrolysates of *Jatropha* hulls with *Klebsiella oxytoca*. *Bioresour. Technol.* **107**, 405–410 (2012).

Acknowledgements

The authors thank the financial support from Chinese Academy of Sciences [CAS 135 program (XTBG-T02) and equipment R&D grant (No. YZ201260)], Yunnan Provincial Government (Baiming Haiwai Gaocengci Rencai Jihua) and Natural Science Foundation of China (No. 31400518). Thanks are also given to the Central Laboratory of Xishuangbanna Tropical Botanical Garden for SEM analysis.

Author Contributions

T.C.S. (PhD student) designed and conducted the experiments, analyzed the data and materials, and wrote the manuscript; Z.F. provided guidance on the manuscript preparation and modified the manuscript and supervised the whole work (supervisor); F.Z. provided important suggestions on the experiments; J.L. modified this manuscript; X.K.L. provided much help on the experiments data analysis. All authors contributed to scientific discussions.

Additional Information

Competing financial interests: The authors declare no competing financial interests.

How to cite this article: Su, T.-C. *et al.* Hydrolysis of Selected Tropical Plant Wastes Catalyzed by a Magnetic Carbonaceous Acid with Microwave. *Sci. Rep.* **5**, 17538; doi: 10.1038/srep17538 (2015).



This work is licensed under a Creative Commons Attribution 4.0 International License. The images or other third party material in this article are included in the article’s Creative Commons license, unless indicated otherwise in the credit line; if the material is not included under the Creative Commons license, users will need to obtain permission from the license holder to reproduce the material. To view a copy of this license, visit <http://creativecommons.org/licenses/by/4.0/>